*Journal of The Electrochemical Society*, **165** (16) A3820-A3827 (2018)
0013-4651/2018/165(16)/A3820/8/$37.00 © The Electrochemical Society

# Theory of Flow Batteries with Fast Homogeneous Chemical Reactions

**Rona Ronen,[1,2] Imri Atlas,[2,3] and Matthew E. Suss[1,2,z]**

[1] *The Nancy & Stephen Grand Technion Energy Program, Technion-Israel Institute of Technology, Haifa 3200003, Israel*
[2] *Faculty of Mechanical Engineering, Technion-Israel Institute of Technology, Haifa 3200003, Israel*
[3] *Russell Berrie Nanotechnology Institute, Technion-Israel Institute of Technology, Haifa 3200003, Israel*

Redox flow batteries are widely investigated toward cost-effective storage of energy generated via intermittent renewable sources. Many redox chemistries have been proposed for flow batteries, possessing various attractive features such as low-cost reactants, fast electrochemical reaction kinetics without precious metal catalysts, negligible thermal runaway risk, and low toxicity. While all flow batteries rely on heterogeneous electrochemical reactions occurring at electrode surfaces, in a subset of chemistries homogeneous chemical reactions occur in the electrolyte. A prominent example are batteries employing halogen-based catholytes, where halogen molecules complex with halide ions in the catholyte, forming redox-active polyhalide ions. However, state-of-the-art models capturing flow battery performance for halogen systems typically neglect the presence of such homogeneous reactions and polyhalide ions. The latter assumption allows for simpler models, but at the cost of accurately predicting battery chemical state and performance. We here present a generalized flow battery theory extended to include fast homogeneous reactions, which employs a technique known as the method of families to simplify the governing equations. We then apply and solve the model for the specific case of a membraneless hydrogen-bromine flow battery, illustrating the predicted effect of the homogeneous complexation reaction in the catholyte on flow battery performance.
 [DOI: 10.1149/2.0251816jes]

Manuscript submitted October 9, 2018; revised manuscript received November 13, 2018. Published December 11, 2018.

To transition grid electricity production from largely fossil fuels to largely intermittent renewable energy sources, such as solar and wind, scalable and cost-effective energy storage solutions are required. One promising solution is the redox flow battery, a rechargeable battery with chemical energy in the form of redox-active chemicals stored in tanks external to the battery, thus spatially decoupling energy storage and power delivery.[1,2] Typically, one tank contains an anolyte with a reducing agent, while a second contains the catholyte with an oxidizing agent. During cell discharge, the anolyte and catholyte are pumped through the battery cell to perform the chemical-to-electrical energy conversion via electrochemical half-reactions at the anode and cathode. The anolyte and catholyte are physically separated by an ionic conductor to prevent direct contact between the reducing and oxidizing agent, typically an ion exchange membrane or third electrolyte flow.[2,3] During cell charging, electric current is applied to the cell to reverse the flow of electrons and regenerate the oxidizing and reducing agent, an electrical-to-chemical energy conversion.

For many redox chemistries promising for flow batteries, homogeneous chemical reactions occur within the catholyte or anolyte flows which can have significant impact on battery performance. For example, in the catholyte of halogen-based flow batteries, diatomic halogen molecules and halide ions react to form polyhalide complexes with often higher solubility than the halogen molecule.[1,4] As battery maximum energy density is proportional to the solubility of the reactant, this complexation reaction is often a key feature underpinning the promise of halogen batteries.[5] Numerous flow batteries employ halogen-based catholytes, including hydrogen-bromine,[3] zinc-bromine,[6] quinone-bromine,[8,13] hydrogen-chlorine,[9] zinc-iodine,[10] and several others.[5,7,11,12] Bromine-based chemistries in particular have been studied extensively due to the low cost of bromine (~$6/kWh),[13] and fast reaction kinetics with no precious metal catalyst required. In bromine-based batteries, the tribromide complex created by the reaction $Br_{2(aq)} + Br^-_{(aq)} \Leftrightarrow Br^-_{3(aq)}$ is often mentioned as a significant oxidizing agent due to the high complexation equilibrium constant of $K_{eq} = 17$,[14–16] while higher order polyhalides are typically neglected due to their lower concentrations in the catholyte.[4,17,18] In addition to polyhalide complexes, other complexes may form in battery electrolytes, such as the zinc-bromide complexes in the anolyte and catholyte of zinc-bromine batteries (e.g. $ZnBr_2$, $ZnBr_3^-$, $ZnBr_4^{-19}$). Non-halide battery chemistries can also rely on homogeneous reactions, for example metal-based batteries relying on the formation of metal ion-ligand complexes.[20–22]

While it is well-known that homogeneous complexation reactions play a crucial role in halogen batteries, recent theoretical models of halogen flow batteries neglected the presence of such reactions.[17,23,24] In these latter models, the diatomic halogen molecule ($Br_2$ or $Cl_2$) is assumed to participate only in the heterogenous electrochemical reaction at the cathode. However, it can be reasonably expected that the predicted battery performance would be significantly affected by accounting for complexation, as polyhalide ions behave differently than the halogen molecule.[25,26] For example, polyhalides are charged and so electromigrate (unlike the halogen molecule), may have different crossover rates than the halogen molecule, and can have different diffusivities and reduction potentials compared to the halogen molecule. Further, both the halogen molecule and polyhalides can be present in significant concentrations in the catholyte simultaneously. Thus, the important coupling between homogeneous reactions and flow battery performance has been largely unexplored, and state-of-the-art models cannot accurately capture the chemical state of the electrolytes and battery performance.

In this work, we provide a general and simplified foundation for modeling flow battery systems with fast homogeneous reactions. For this, we adapt a methodology commonly used to model microfluidic separation processes in the presence of homogeneous reactions involving protonation or deprotonation of ampholytes,[27] known as the method of families.[28] In such systems, the "family" typically refers to all ionization states of the ampholyte present in the electrolyte, and the method relies on recognizing mass conservation of all species within the family.[27] This method was later extended in several ways, for example to include homogeneous complexation equilibria of analytes with ligands,[29] and to describe systems with non-equilibrium homogeneous and surface heterogeneous binding or hybridization-type reactions involving biomolecules.[30] A similar method has been used to model electrochemical systems with fast homogeneous reactions, such as ion exchangers,[31] $CO_2$ capture and mixing energy harvesting using capacitive electrodes,[32] and bioelectrochemical cells (albeit without accounting for the effect of electrode reaction kinetics).[33] To the best of our knowledge, this method has not previously been extended to describe a system with both homogeneous reactions in the electrolyte and heterogeneous electrochemical reactions occurring at electrodes, including the electrochemical reaction kinetics, which is necessary for modeling flow batteries. After presenting the general form of the model, we apply the model to the specific case of a

[z] E-mail: mesuss@technion.ac.il

membraneless flow battery with $H_2/Br_2$ chemistry. We compared the results of the latter model including homogeneous complexation reactions to an identical model but without complexation, in order to elucidate the coupling between the homogeneous reaction and flow battery performance. In the future, the approach described here can be used for improved model-to-data comparisons on the performance and chemical state of halogen batteries and other batteries with homogeneous reactions, and aid in advanced battery design.

## Theory

***Generalized model formulation.—***We here develop the equations for modelling a redox flow battery with planar electrodes including homogeneous reactions in the electrolyte. In the dilute limit,[17,24,34] the fluxes due to electromigration, diffusion and advection are linearly superposable and given by the Nernst-Planck equation,

$$\vec{N}_{i,k} = -D_{i,k}\nabla c_{i,k} + \vec{u}c_{i,k} - \mu_{i,k}c_{i,k}\nabla\varphi \quad i = 1...N,\ k = n_i...p_i. \tag{1}$$

Here $\varphi$ is the electric potential, $\vec{u}$ is the fluid velocity, and $c_{i,k}$,$D_{i,k}$,$\mu_{i,k}$ are, respectively, the concentration, molecular diffusivity and ionic mobility of a species $k$ which belongs to family $i$. In the microfluidic literature,[27,28,35] the term "family" typically refers to all charge states of a given ampholyte present in the electrolyte. However, in flow batteries the homogenous reactions of interest are not limited to ampholytes with protonation/deprotonation-type reactions, but often include complexation reactions such as $Br_2 + Br^- \Leftrightarrow Br_3^-$. Thus, we here use the term "family" to refer to all species containing a given atom (e.g. Br), and note that different species in the family may have the same valence (e.g. $Br^-$ and $Br_3^-$). We designate that the subscript $k$ refers to the number of atoms per species (e.g. for $Br_2$, $k = 2$). Further, $N$ is the total number of families, and $n_i$ and $p_i$ are, respectively, the minimum and maximum number of atoms common to the family $i$ contained in a species belonging to the family (e.g. $n_{Br} = 1$ for $Br^-$, and $p_{Br} = 3$ for $Br_3^-$ when neglecting higher order polybromides). For ampholytes, the same Equation 1 can still be used, but by reverting to the classic definition of "family" and with the ion valence $z$ replacing the subscript $k$.[27,28] A mass conservation applied to each species belonging to a family yields

$$\frac{\partial c_{i,k}}{\partial t} + \nabla\cdot\left(-D_{i,k}\nabla c_{i,k} + \vec{u}c_{i,k} - \mu_{i,k}c_{i,k}\nabla\varphi\right) - R_{i,k} = 0 \quad i = 1...N,\ k = n_i...p_i, \tag{2}$$

where $R_{i,k}$ is the production rate of species $k$ belonging to family $i$ due to local homogeneous reactions. To apply the method of families to our system, we multiply each mass conservation equation by the index $k$, and sum all modified conservation equations associated with the family $i$, to obtain:

$$\frac{\partial}{\partial t}\sum_{k=n_i}^{p_i} kc_{i,k} + \nabla\cdot\left(-\sum_{k=n_i}^{p_i} kD_{i,k}\nabla c_{i,k} + \vec{u}\sum_{k=n_i}^{p_i} kc_{i,k} - \left(\sum_{k=n_i}^{p_i} k\mu_{i,k}c_{i,k}\right)\nabla\varphi\right) - \sum_{k=n_i}^{p_i} kR_{i,k} = 0 \quad i = 1...N,\ k = n_i...p_i. \tag{3}$$

Eq. 3 can be interpreted as a transport equation for the atom common to the family (e.g. a transport equation for Br), and can be simplified by noting that the local production rate of the atom must be zero, $\sum_{k=n_i}^{p_i} kR_{i,k} = 0$. This is an important simplification yielded by the method of families, as here reaction rate constants do not need to be specified in the transport equations. By contrast, several works modeling $Br_2/Br^-$ rotating disk electrodes and zinc-bromine electrochemical cells consider homogeneous complexation reactions, but specify reaction rates in the transport equations.[25,36,37] Additionally, Evans and White[37] eliminated the production terms due to homogeneous reactions from the transport equations, but presented a model specific to zinc-bromine batteries which contained several transport equations for species containing Br atoms rather than a single family transport equation.

Eq. 3 may now be re-written in more compact notation as

$$\frac{\partial C_i}{\partial t} + \nabla\cdot\left[-D_i\nabla C_i + \vec{u}C_i - \mu_i C_i\nabla\varphi\right] = 0 \quad i = 1...N, \tag{4}$$

where $C_i$ is a conserved scalar representing the total concentration of the family $i$, defined as:

$$C_i = \sum_{k=n_i}^{p_i} kc_{i,k} \quad i = 1...N. \tag{5}$$

Further, $D_i$ is an effective diffusion coefficient, which is defined using the diffusion flux of the family i, $\vec{N}_{diff,i}$

$$\vec{N}_{diff,i} = \sum_{k=n_i}^{p_i} kD_{i,k}\nabla c_{i,k} \equiv D_i\nabla C_i. \tag{6}$$

$D_i$ can also be interpreted as the local weighted mean of the diffusivities of the species in family $i$,[30] and thus typically $D_i$ is not uniform in space, even with constant values of $D_{i,k}$. Similarly, $\mu_i$ is an effective ion mobility, which is defined by considering the electromigration flux of the family,

$$\vec{N}_{em,i} = \left(\sum_{k=n_i}^{p_i} k\mu_{i,k}c_{i,k}\right)\nabla\varphi \equiv \mu_i C_i\nabla\varphi. \tag{7}$$

By applying the Einstein relation, $\mu_{i,k} = z_{i,k}D_{i,k}{}^{F}/_{RT}$, where $z_{i,k}$ is the species valence, $R$ is the ideal gas constant, $T$ is the temperature, and $F$ is Faraday's constant, the effective mobility can be written in terms of molecular diffusivities,

$$\mu_i = \frac{F}{RT}\frac{\sum_{k=n_i}^{p_i} kz_{i,k}D_{i,k}c_{i,k}}{C_i}. \tag{8}$$

Since the family approach reduces the number of transport equations per family to one, additional relations are required to close the system. The charge balance equation can be written as

$$F\sum_j z_j\left(\frac{\partial c_j}{\partial t} + \nabla\cdot\vec{N}_j\right) = 0, \tag{9}$$

Where the $j$ index represents each of the chemical species present in the system. Assuming steady state or invoking electroneutrality, $\sum_j z_j c_j = 0$, reduces Eq. 9 to $\nabla\cdot\vec{J} = 0$, where $\vec{J}$ the ionic current density in solution, given by $\vec{J} = F\sum_j z_j\vec{N}_j$. In the limit of fast homogeneous reactions, such that chemical equilibrium applies throughout the model domain, we can write

$$K_{i,m} = \frac{\prod_{\text{Products}}\tilde{c}_{i,k}^{s_{i,k}}}{\prod_{\text{Reactants}}\tilde{c}_{i,k}^{s_{i,k}}}, \tag{10}$$

where $K_{i,m}$ is the equilibrium constant for the homogeneous reaction $m$ involving family $i$, $s_{i,k}$ is the stochiometric coefficient of species $k$ from family $i$, and $\tilde{c}$ represents concentration normalized by a reference concentration, $c_{ref} = 1$ M. The assumption of fast homogeneous reactions is commonly invoked in models of electrochemical and electrokinetic systems,[25,27,32,33,37] and allows for simplifying the theory, but can be relaxed in a future work without invalidating Eq. 4. The remaining components of the theory, such as electrode boundary conditions, are developed in the following sections for the specific case of a $H_2$-$Br_2$ battery.

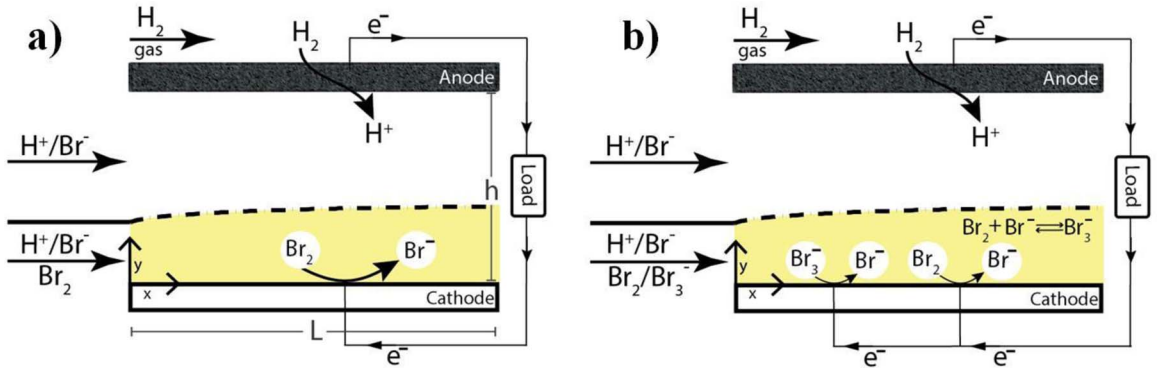


**Figure 1.** Schematics of the model system in discharge mode, for (a) the model when neglecting complexation,[17] and (b) our model including the complexation reaction $Br_2 + Br^- \Leftrightarrow Br_3^-$ in the catholyte and both bromine and tribromide reduction at the cathode. The anode and cathode are planar electrodes, and side-by-side laminar flows of catholyte (shown in yellow) and electrolyte (HBr, colorless) prevent the crossover of $Br_2$ and $Br_3^-$ to the anode.

***Method of families applied to a membraneless $H_2$-$Br_2$ redox flow battery.***—We now develop the model given in Generalized model formulation section further, and apply it to the specific case of a $H_2$-$Br_2$ membraneless redox flow battery with planar electrodes (see Figure 1). In such a cell, a laminar flow of hydrobromic acid (HBr) electrolyte physically separates the catholyte from the anode to prevent crossover of $Br_2$ and $Br_3^-$.[17] Unlike recent models of $H_2$-$Br_2$ flow batteries (Figure 1a),[17,24,38] we here account for the complexation reaction occurring in the catholyte, $Br_2 + Br^- \Leftrightarrow Br_3^-$, and the reduction of $Br_3^-$ at the cathode (Figure 1b). As tribromide is expected to be the dominant polybromide in the catholyte, see Section SI-3, complexation reactions forming higher order polybromides ($Br_5^-$, $Br_7^-$) will be neglected here, but can be incorporated in the future using the generalized equations in Generalized model formulation section. We here assume steady-state, 2-D geometry, and 1-D Poiseuille flow between the electrodes according to $u_x = 6U(y/h - y^2/h^2)$ where $U$ is the mean velocity, and $h$ is the distance between electrodes. For a thin channel where $L >> h$, we can neglect species electromigration and diffusion in the $x$-direction (as is common in both flow batteries and electrodialysis cells).[39,40] Applying Eq. 4 to the bromine family, we obtain:

$$u_x \frac{\partial C_{Br}}{\partial x} = \frac{\partial}{\partial y}\left[D_{Br}\frac{\partial C_{Br}}{\partial y} + \mu_{Br} C_{Br}\frac{\partial \varphi}{\partial y}\right], \qquad [11]$$

Where $C_{Br}$ is the total concentration of the bromine family, and is given by Eq. 5 as

$$C_{Br} = c_{Br^-} + 2c_{Br_2} + 3c_{Br_3^-}. \qquad [12]$$

Here, $c_{Br^-}$, $c_{Br_2}$, and $c_{Br_3^-}$, are the concentrations of bromide, bromine, and tribromide species respectively. Applying Eq. 6 we obtain

$$D_{Br}\frac{\partial C_{Br}}{\partial y} = D_{Br^-}\frac{\partial c_{Br^-}}{\partial y} + 2D_{Br_2}\frac{\partial c_{Br_2}}{\partial y} + 3D_{Br_3^-}\frac{\partial c_{Br_3^-}}{\partial y}, \qquad [13]$$

and using Eqs. 8

$$\mu_{Br} = -\frac{F}{RT}\left[D_{Br^-}c_{Br^-} + 3D_{Br_3^-}c_{Br_3^-}\right]. \qquad [14]$$

Substituting Eqs. 12, 13 and 14 into Eq. 11, and scaling the potential $\varphi$ by the thermal voltage, $RT/F$, to obtain a dimensionless voltage, $\tilde{\varphi}$, yields

$$u_x \frac{\partial}{\partial x}\left(c_{Br^-} + 2c_{Br_2} + 3c_{Br_3^-}\right) = \frac{\partial}{\partial y}\left(D_{Br^-}\frac{\partial c_{Br^-}}{\partial y} + 2D_{Br_2}\frac{\partial c_{Br_2}}{\partial y} + 3D_{Br_3^-}\frac{\partial c_{Br_3^-}}{\partial y} - \left(D_{Br^-}c_{Br^-} + 3D_{Br_3^-}c_{Br_3^-}\right)\frac{\partial \tilde{\varphi}}{\partial y}\right). \qquad [15]$$

By replacing $c_{Br^-}$ and $c_{Br_2}$ in the above equation using electroneutrality, $\tilde{c}_{Br^-} = (\tilde{c}_{H^+} - \tilde{c}_{Br_3^-})$, and the equilibrium expression Eq. 10, $\tilde{c}_{Br_2} = \tilde{c}_{Br_3^-}/K(\tilde{c}_{H^+} - \tilde{c}_{Br_3^-})$, where $K$ is given in Table I, we obtain an equation that depends only on $c_{H^+}$, $c_{Br_3^-}$ and $\tilde{\varphi}$. Suss et al. presented a variation of this equation for a cell without electrochemical reactions in order to study crossover of various species in a membraneless $H_2$-$Br_2$ cell.[41] The hydronium ion is not included in the bromine family, and thus we need a hydronium ion transport equation, given by

$$u_x \frac{\partial \tilde{c}_{H^+}}{\partial x} = D_{H^+}\frac{\partial}{\partial y}\left(\frac{\partial \tilde{c}_{H^+}}{\partial y} + \tilde{c}_{H^+}\frac{\partial \tilde{\varphi}}{\partial y}\right). \qquad [16]$$

Note that in our system, the electrolyte is strongly acidic, so that we neglected the presence of $OH^-$ due to its very low concentration, and the effect of water self-ionization on the $H^+$ mass balance (Eq. 16). However, the method of families approach used here can in the future be extended to include water self-ionization (a homogenous reaction),[28,42] and this may be most relevant for cells with near-neutral pH electrolytes (e.g. zinc-bromine batteries).

**Table I. Model parameters.**

| Parameter | Symbol | Value |
|---|---|---|
| Inlet catholyte bromine concentration | $\tilde{c}^{cat}_{Br_2}$ | 0.22 |
| Inlet catholyte tribromide concentration | $\tilde{c}^{cat}_{Br_3^-}$ | 0.78 |
| Inlet catholyte bromide concentration | $\tilde{c}^{cat}_{Br^-}$ | 0.22 |
| Inlet electrolyte bromide concentration | $\tilde{c}^{el}_{Br^-}$ | 1 |
| Inlet hydronium ion concentration | $\tilde{c}_o$ | 1 |
| Temperature | $T$ | 298 K |
| Bromide diffusivity | $D_{Br^-}$ | $2.08 \times 10^{-5}$ cm$^2$ s$^{-1}$ |
| Bromine diffusivity | $D_{Br_2}$ | $1.15 \times 10^{-5}$ cm$^2$ s$^{-1}$ |
| Tribromide diffusivity | $D_{Br_3^-}$ | $1.15 \times 10^{-5}$ cm$^2$ s$^{-1}$ |
| Hydronium diffusivity | $D_{H^+}$ | $9.3 \times 10^{-5}$ cm$^2$ s$^{-1}$ |
| Channel length | $L$ | 1.3 cm |
| Catholyte flow thickness at inlet* | $h_{ca}$ | $2 \times 10^{-4}$ m |
| Electrolyte flow thickness at inlet* | $h_{el}$ | $6 \times 10^{-4}$ m |
| Complexation equilibrium constant | $K$ | 16.7[14] |
| Mean flow velocity | $U$ | 1.44 cm s$^{-1}$ |
| Anode exchange current density | $J_{o,a}$ | 0.5 A cm$^{-2}$[17] |
| Cathode exchange current density | $J_{o,c}$ | 0.5 A cm$^{-2}$ [17] |
| Standard reduction potential, $Br_2/Br^-$ | $\Delta\varphi^0_{c,Br_2}$ | 42.3 (1.087 V) |
| Standard reduction potential, $H_2/H^+$ | $\Delta\varphi^0_a$ | 0 (0 V) |

*Channel height is $h = h_{ca} + h_{el} = 800\mu$m.

For our system, the charge balance equation, $\nabla \cdot \vec{J} = 0$, can be written as

$$\nabla \cdot \left[ \left(D_{Br^-} - D_{H^+}\right) \nabla \tilde{c}_{H^+} + \left(D_{Br_3^-} - D_{Br^-}\right) \nabla \tilde{c}_{Br_3^-} + \left[ \left(D_{Br^-} - D_{H^+}\right) \tilde{c}_{H^+} + \left(D_{Br_3^-} - D_{Br^-}\right) \tilde{c}_{Br_3^-} \right] \nabla \tilde{\varphi} \right] = 0. \quad [17]$$

Eq. 15, Eq. 16 and Eq. 17, form a coupled system of equations which can be solved for $\tilde{c}_{H^+}$, $\tilde{c}_{Br_3^-}$, and $\tilde{\varphi}$. Subsequently, $\tilde{c}_{Br^-}$ and $\tilde{c}_{Br_2}$ can be obtained via the electroneutrality expression and reaction equilibrium expression, respectively.

***Boundary conditions for $H_2$-$Br_2$ electrochemical cells.***—In our model, we account for hydrogen oxidation at the anode and both bromine and tribromide reduction at the cathode,[43]

$$H_2 \rightarrow 2H^+ + 2e^-, \quad [18]$$

$$Br_2 + 2e^- \rightarrow 2Br^-, \quad [19]$$

$$Br_3^- + 2e^- \rightarrow 3Br^-. \quad [20]$$

These reactions are for the discharge mode of the cell, and are reversed during cell charging. Side reactions during cell charging such as hydrogen and oxygen evolution are not considered here, and neither are reactions due to possible crossover of bromine and tribromide to the anode. To describe the current due to electrochemical reactions occurring at the planar electrodes, which form two boundaries of our model domain (Figure 1), we use the symmetric Butler-Volmer equation (symmetric transfer coefficient, $\alpha = 0.5$[17,44]),

$$j = 2J_o \sqrt{\tilde{c}_{ox}\tilde{c}_{red}} \sinh\left(\frac{nF\eta}{2RT}\right). \quad [21]$$

The electrode overpotential, $\eta$, is defined by $\eta \equiv \Delta\varphi - \Delta\varphi^{eq}$, where $\Delta\varphi$ is the potential drop across the solid-liquid interface, and the superscript $eq$ refers to equilibrium. Further, $\tilde{c}_{ox} \equiv \prod_{ox} \tilde{c}_{i,ox}^{s_i,ox}$ and $\tilde{c}_{red} \equiv \prod_{red} \tilde{c}_{i,red}^{s_i,red}$ represent the dimensionless surface concentrations of the oxidized and reduced states at the electrode, $s_i$ are the stoichiometric coefficients, and $J_o$ is an exchange current density. For the redox half-reactions in our system, the overpotentials at the anode and cathode can be written as

$$\eta_a = \varphi_a^s - \varphi_a - \Delta\varphi_a^{eq}, \quad [22]$$

$$\eta_c = \varphi_c^s - \varphi_c - \Delta\varphi_c^{eq}, \quad [23]$$

where $\varphi^s$ denotes the electrode potential, and $\varphi_a$, $\varphi_c$ denote the electrolyte potential at the location of the anode and cathode, respectively. In our cell, we consider the anode to be grounded, and thus the electrode potentials are $\varphi_a^s = 0$, $\varphi_c^s = V_{cell}$. We express a dimensionless $\Delta\varphi^{eq}$ via the Nernst equation, and assume unity activity of hydrogen gas at the anode, as is appropriate for a surplus supply of atmospheric pressure $H_2$ gas. Thus, the relevant Nernst equations are

$$\Delta\varphi_a^{eq} = \Delta\varphi_a^0 + \ln \tilde{c}_{H^+}, \quad [24]$$

$$\Delta\varphi_c^{eq} = \Delta\varphi_{c,Br_2}^0 + \frac{1}{2} \ln\left(\frac{\tilde{c}_{Br_2}}{\tilde{c}_{Br^-}^2}\right). \quad [25]$$

Here $\Delta\varphi_a^0$, $\Delta\varphi_{c,Br_2}^0$ are the dimensionless standard potentials for hydrogen and bromine reduction, respectively. Note that Eq. 25 is based on bromine reduction, but could equivalently be predicted by considering instead tribromide reduction (see SI-1). While the expression for cathode Nernst potential, Eqs. 25, is identical to that in models which neglect complexation,[17] it is important to recognize that the values of the concentrations of $Br_2$ and $Br^-$ at equilibrium are affected by complexation. Combining Eqs. 21, 22 and 24, we obtain an expression for current at the anode,

$$j_a = -2J_{o,a}\tilde{c}_{H^+} \sinh\left[\tilde{\varphi}(y = h) + \Delta\varphi_a^{eq}\right]. \quad [26]$$

For the cathode, we have two electroactive species, bromine and tribromide, which are coupled at the cathode solution-side via the fast homogeneous complexation reaction. Previous theoretical works assumed that only $Br_2$ was active at the interface, and $Br_3^-$ then served as a chemical source of $Br_2$ at the cathode during discharge.[25,45] We here relax this assumption and explore system performance when describing the reduction of $Br_2$ (Eq. 19) and $Br_3^-$ (Eq. 20) each by a separate Butler-Volmer equation (see SI-2). This leads to following expression for current at the cathode,

$$j_c = -2J_{o,c}\tilde{c}_{Br^-}\sqrt{\tilde{c}_{Br_2}}\left(1 + \tilde{c}_{Br^-}\sqrt{K}\right) \times \sinh\left[\tilde{\varphi}(y = 0) - V_{cell}\,(F/RT) + \Delta\varphi_c^{eq}\right]. \quad [27]$$

At the cathode boundary of our model, we implemented current conservation across the electrode/electrolyte interface, $j_c = \hat{n} \cdot \vec{J}$ ($\hat{n}$ is the outwards pointing normal vector), zero bromine (Br) flux, $\hat{n} \cdot \sum_{k=1}^{3} k\vec{N}_{Br_f,k} = 0$, and zero flux of $H^+$, $\hat{n} \cdot \vec{N}_{H^+} = 0$. At the anode boundary, we implemented $j_a = \hat{n} \cdot \vec{J}$, $\hat{n} \cdot \sum_{k=1}^{3} k\vec{N}_{Br_f,k} = 0$, and $\hat{n} \cdot \vec{N}_{H^+} = j_a/F$. The inlet boundary conditions involve specified species concentrations which enter the battery from the upstream electrolyte and catholyte tank,

$$\tilde{c}_{H^+}(x = 0) = \tilde{c}_o \quad [28]$$

$$\tilde{c}_k\,(x = 0) = \begin{cases} \tilde{c}_k^{cat} & y < 0.2h \\ \tilde{c}_k^{el} & 0.2h < y \end{cases}, \quad [29]$$

where $\tilde{c}_k^{cat}$ and $\tilde{c}_k^{el}$ are the dimensionless catholyte and electrolyte concentrations, and $0.2h$ represents the thickness of the catholyte flow at the inlet of the membraneless cell (see Figure 1). During flow battery operation, often the inlet concentrations of electroactive species vary significantly in time as these species are depleted or replenished in the battery, and then returned to the tank and subsequently the battery inlet. Here we neglect this effect in order to focus on the effects of complexation over shallow battery cycling, but in the future the boundary conditions and model equations can be updated to capture time-dependent effects due to deeper cycling. To obtain $\tilde{c}_k^{cat}$, we solved for the concentrations of all bromine containing species at equilibrium given a solution of 1 M $Br_2$ and 1 M HBr pre-complexation, see Figure S2. At both the upstream and downstream boundaries, we assume zero ionic current, and downstream we set the flux of each species to that provided by local advection. 2D simulations were performed in the finite element framework of COMSOL Multiphysics, where direct solver MUMPS was used. A triangular mesh with number of elements of 110,432 was used.

## Results and Discussion

In Table I, we list the parameters used in the model given by Eqs. 15 to 17. The parameters defining channel geometry, exchange current densities, catholyte flow thickness, and flow velocity were those used in Braff et al.[17] In Figure 2 we show the computed solution to the model given by Eqs. 15–17, plotting predicted normalized species concentrations (divided by inlet values given in Table I), for the case of the battery discharging at $V_{cell} = 0.9$ V. At this cell voltage, the concentration of both $Br_2$ and $Br_3^-$ are observed to approach zero at the cathode (Figure 2a and 2b), and thus the battery is at its maximum discharge current (limiting current). We can further see that a concentration boundary layer develops near the cathode due to consumption of $Br_2$ and $Br_3^-$ and production of $Br^-$. The depletion

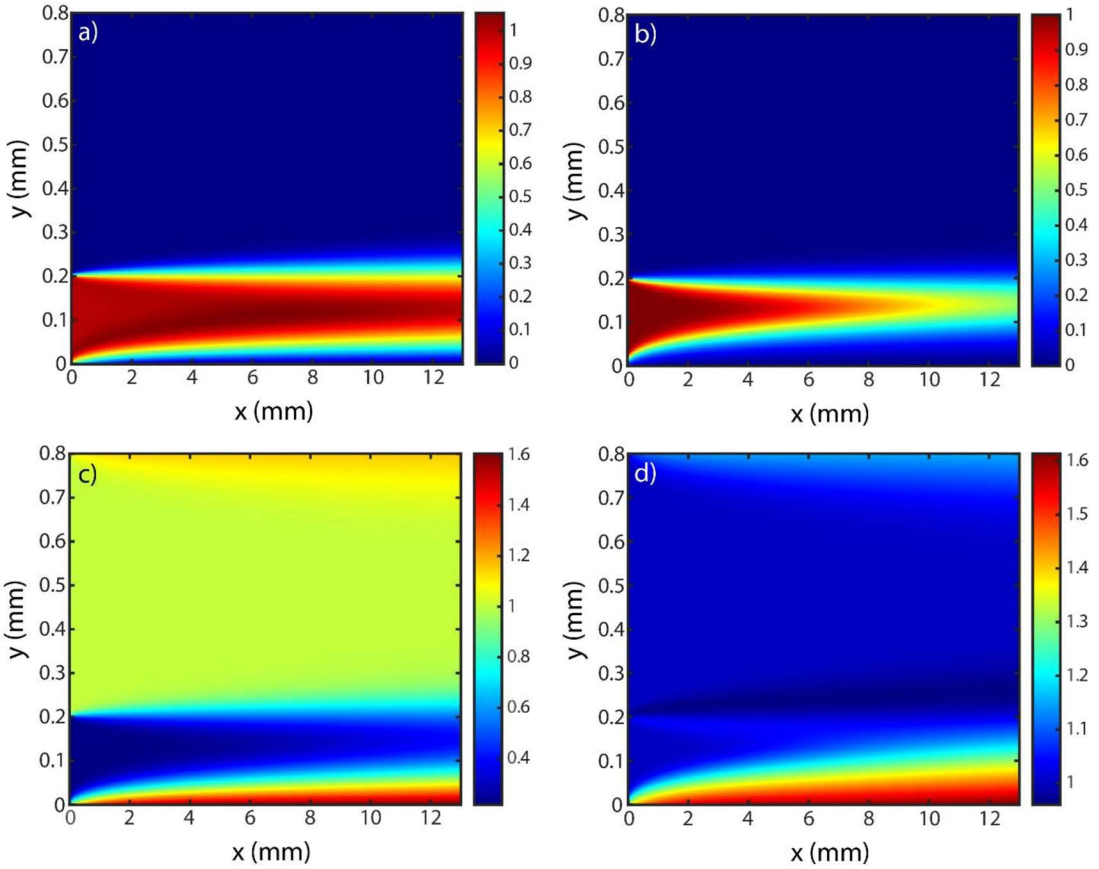


**Figure 2.** Predicted normalized concentration distributions of all species present in the model system, a) $c_{Br_3^-}/c^{cat}_{Br_3^-}$ b) $c_{Br_2}/c^{cat}_{Br_2}$, c) $c_{Br^-}/c^{el}_{Br^-}$, and d) $c_{H^+}/c_o$, for the parameters used in Table I and $V_{cell} = 0.9$ V. The colorbar indicates the normalized concentration value.

boundary layers formed at the cathode are of particular interest. In models neglecting complexation the $Br_2$ boundary layer determines the maximum transport rate of reactant from the bulk catholyte to the cathode and thus the limiting current achievable by the battery.[17] In comparing Figures 2a and 2b, a distinct difference in the $Br_2$ and $Br_3^-$ boundary layers is observed, with $Br_3^-$ concentration appearing markedly higher relative to its inlet value at most locations, despite equal diffusivities between these species (see Table I). In addition, the normalized concentration of $Br_3^-$ at areas within the catholyte rises above unity (above the inlet concentration), meaning that there is a significant source of $Br_3^-$ in the catholyte during discharge due to the homogeneous complexation reaction. Thus, the latter observations demonstrate that the concentration field within the boundary layer at the cathode is not determined solely by a balance between diffusion to the cathode and advection along the cathode, as predicted when complexation is neglected,[17] but that there is an important role of complexation. The $Br_3^-$ ion is charged and thus also subject to electromigration, but this accounts for only ~1.5% of the total flux of $Br_3^-$ at the cathode surface at these model conditions. Another notable feature in Figure 2 is a mixing zone which develops between the electrolyte and catholyte flows due to the membraneless design. As expected, $Br_2$ and $Br_3^-$ diffuse from the catholyte to the electrolyte,[17] but also $Br^-$ diffuses from the electrolyte to the catholyte. Such $Br^-$ diffusion occurs because this species is depleted in the catholyte due to the complexation reaction (Figure 2c). Further, in Figure 2d, a thin, slight depletion layer of $H^+$ is present at the upper half of the mixing layer (just above y = 0.2 mm), while a slight enrichment layer is present at the lower half (just below y = 0.2 mm). The latter feature is due to the cross-diffusion of $Br^-$ and $Br_3^-$ through the mixing layer, where $Br^-$ has higher diffusivity, resulting in a net flux of $H^+$ from the upper half to the lower half of the mixing zone to maintain electroneutrality.

In Figure 3, we again show the solution to the model, but now for $V_{cell} = 1.2$ V, so that the cell is in charging mode. Distinct differences between the concentration fields of $Br_2$ and $Br_3^-$ in the catholyte are observed (Figures 3a and 3b). Bromine is largely enriched in the catholyte, with concentrations reaching three times higher than the inlet concentration, while $Br_3^-$ concentration is largely unchanged, and is even slightly depleted at the cathode surface. The $Br_3^-$ concentration field thus yields counter-intuitive results, as $Br_3^-$ is electrochemically produced at the cathode during charging, so naively we may expect it should be enriched near to the cathode surface. Bromide shows a near zero concentration at the cathode surface, indicating we should expect a significant mass-transport overpotential at this charging voltage (Figure 3c). The hydronium ion by contrast is only slightly depleted at the anode (Figure 3d), is also depleted at the cathode, and demonstrates slight enrichment and depletion layers at the mixing zone between catholyte and electrolyte (although reversed in orientation compared to Figure 2d).

While Figures 2 and 3 showed predicted concentration fields for a given value of $V_{cell}$, we now investigate the predicted battery performance over a wide range of $V_{cell}$ in the form of a polarization curve. In Figure 4, we plot both a predicted polarization curve for the case where complexation was neglected (dotted line), and a predicted polarization curve from our model when including complexation (solid line). Both cases used the parameters listed in Table I, except when neglecting complexation we used inlet conditions for the catholyte of 1M HBr and 1M $Br_2$. Positive current density is defined for the discharge mode, whereas the negative current density is for the charging mode. From Figure 4, we can see several distinct differences

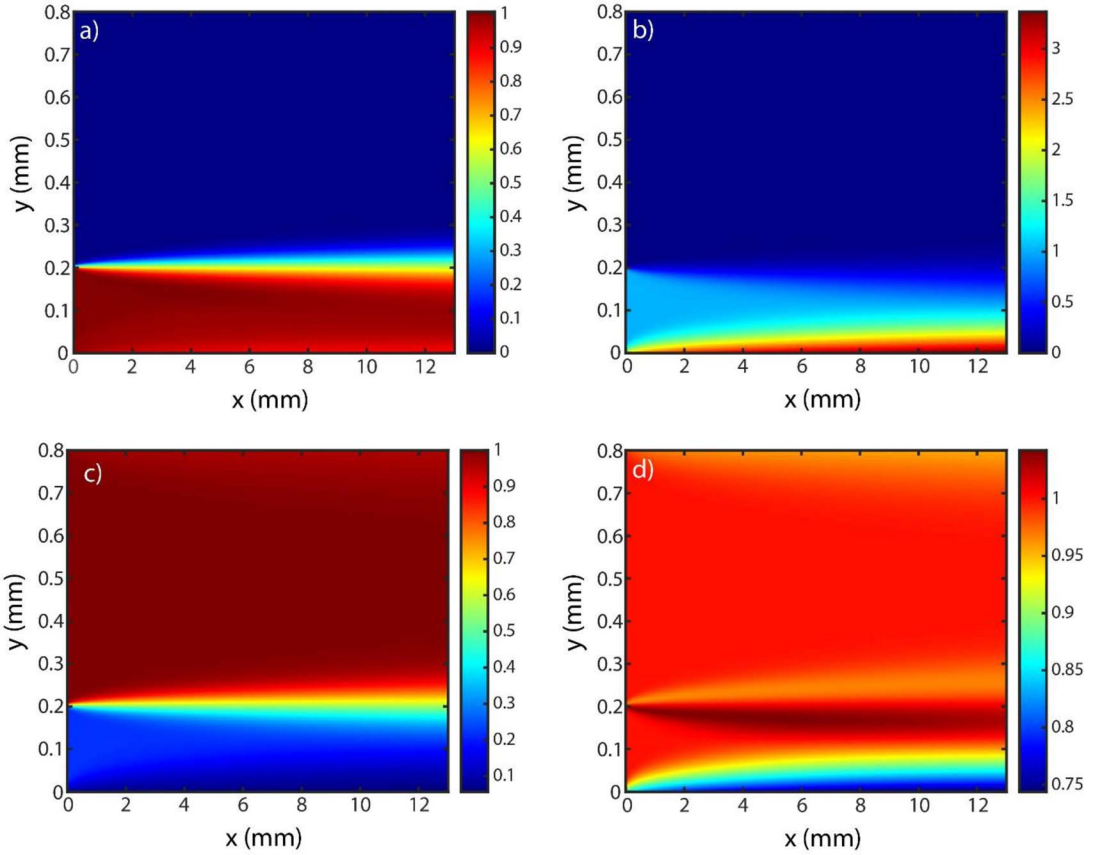


**Figure 3.** Predicted steady-state concentration distributions of all species present in the model system , a) $c_{Br_3^-}/c^{cat}_{Br_3^-}$ b) $c_{Br_2}/c^{cat}_{Br_2}$, c) $c_{Br^-}/c^{el}_{Br^-}$, and d) $c_{H^+}/c_o$, for the parameters used in Tables I and $V_{cell} = 1.2$ V. The colorbar indicates the normalized concentration value.

between the two model predictions, highlighting the important role the complexation reaction is expected to play in determining battery performance. One notable feature in Figure 4 is that from between about 100–300 mA cm$^{-2}$ both polarization curves are approximately

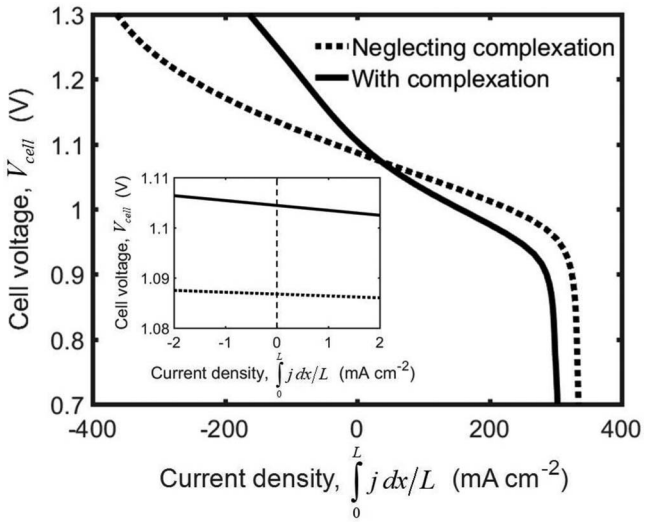


**Figure 4.** Predicted polarization curves for our model including complexation (solid line) and an identical model except which neglects complexation (dashed line). Accounting for complexation leads to a reduction in predicted limiting current, higher cell resistance, higher open circuit potential (inset) and higher voltage upon cell charging.

linear, indicating that for those currents the slope of the curve is largely due to electrolyte ohmic losses. The model with complexation shows a steeper slope in this region, relative to that neglecting complexation, which indicates a higher resistance when accounting for complexation. This can be attributed largely to the lower catholyte ionic conductivity when accounting for complexation. The ionic conductivity of the catholyte is given by $\sigma = \sum_j {z_j}^2 F^2 D_j c_j / RT$, where the index $j$ sums over all species present in the catholyte. For a 1M HBr/$Br_2$ catholyte neglecting complexation, the calculated conductivity is 0.428 S/cm, whereas it is 0.4 S/cm after complexation as much of the $Br^-$ is converted to lower diffusivity $Br_3^-$.

Another notable feature in Figure 4 is the significantly higher voltage for the model with complexation at all charging currents. For example, at $-100$ mA/cm$^2$, the model without complexation predicts a cell voltage of 1.126 V, while that with complexation predicts 1.223 V. During charging, at the cathode $Br_2$ and $Br_3^-$ are generated and $Br^-$ consumed. The higher charging voltage can be largely attributed to higher mass transport losses at the cathode, caused by lower bromide concentrations in the catholyte when including complexation, where the average concentration at the cathode is 0.05 M with complexation and 0.16 M when neglecting complexation. Additionally, the open circuit voltage (OCV) for the model with complexation is noticeably higher, 1.104 V vs. 1.087 V, (see Figure 4 inset), which can also be predicted by the Nernst equation, Eq. 25, when accounting for significantly lower bromide and bromine concentrations due to complexation (see also SI-1). Figure 4 also shows that including complexation results in a lower predicted limiting current on discharge, where the model with complexation predicts about 303 mA cm$^{-2}$, while neglecting complexation shows a limiting current of approximately 334 mA cm$^{-2}$. Limiting current occurs when reactant

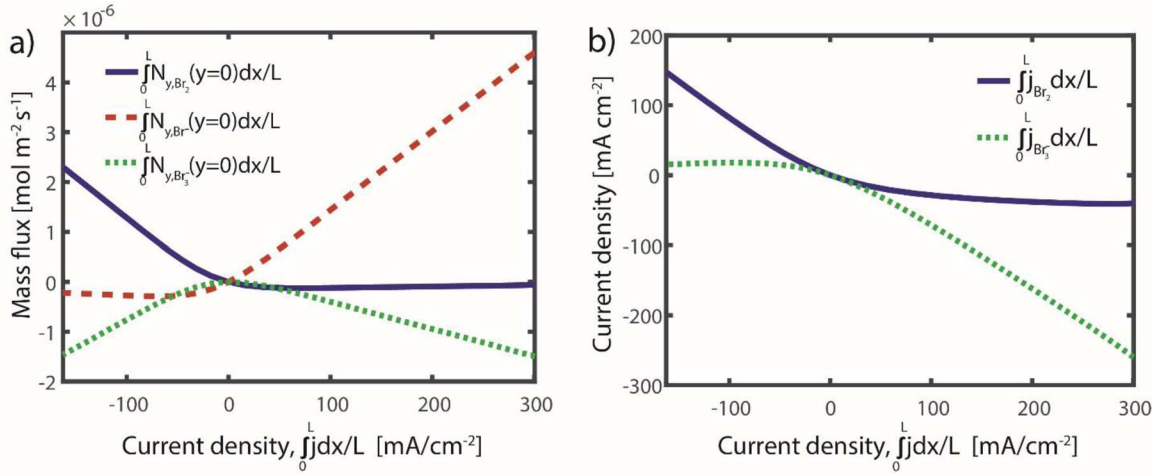


**Figure 5.** a) Model predictions for total mass flux at the cathode for each species in the bromine family, versus cell current density. b) Model predictions for cathode current density associated with bromine or tribromide versus cell current density.

concentration at the cathode surface approaches zero. In the model without complexation, this occurs when transport of reactant to the cathode is maximized, where this transport is due solely to diffusion of $Br_2$ to the cathode surface.[17] When including complexation, limiting current is determined by several effects, including both $Br_2$ and $Br_3^-$ diffusion to the cathode, electromigration of $Br_3^-$ away from the cathode, and the coupling of $Br_2$ and $Br_3^-$ via the complexation reaction. Thus, this observed variation in limiting current suggests that future boundary layer analysis for predicting limiting current should account for complexation effects.

We return to the counter-intuitive result shown in Figure 3a, where the tribromide concentration at the cathode was slightly depleted relative to the inlet concentration during cell charging. To probe deeper into this observation, in Figure 5a, we show predicted mass flux of all species included in the bromine family ($Br_2$, $Br_3^-$, $Br^-$) at the cathode versus cell current density. Positive mass flux represents flux directed away from the cathode, while negative mass flux is toward the cathode. As can be seen, bromine transport is overall toward the cathode during discharging and away during charging (solid line in Figure 5a), corresponding with the direction of bromine current (solid line in Figure 5b). Additionally, bromide transports toward the cathode during charging and away during discharging (dashed line in Figure 5a), as expected based on its electrochemical production at the cathode during discharge and utilization during charge. By contrast, we can see that tribromide is always transported toward the cathode, at all cell currents tested, both for cell charging and discharging (dotted line in Figure 5a). This is despite the electrochemical production of tribromide at the cathode during charging (dotted line in Figure 5b). The latter observation points to the strong impact of the complexation reaction, as tribromide depletion at the cathode must occur because the complexation reaction consumes tribromide at a higher rate than it is produced electrochemically. The complexation reaction is directed toward tribromide consumption during charging largely to supply bromide to the cathode.

## Conclusions

We here present a general modeling framework for flow batteries with fast homogeneous reactions, and develop the model toward the specific example of a membraneless $H_2$-$Br_2$ cell. By applying the method of families, we are able to simplify the system of equations to three coupled partial differential equations without homogeneous reaction terms, Eqs. 15–17, which were solved numerically. We presented results for the example cell when neglecting bromine/bromide complexation and when including complexation, in order to elucidate the important effects of this homogeneous complexation reaction on the predicted battery performance. In the future, this model framework can be applied broadly to flow batteries with homogeneous reactions, and should be validated with a dedicated set of experimental results of battery performance and reactant stream chemical state.

## Acknowledgments

The authors acknowledge financial support from Israel Chemicals Ltd (ICL). A partial support for this work was obtained from the Israeli Committee of High Education and the Israeli Prime Minister office via the INREP project. This study is Supported by The Nancy and Stephen Grand Technion Energy Program (GTEP) and the Ministry of National Infrastructures, Energy and Water Resources via graduate student scholarships in the energy fields. Imri Atlas acknowledges the support of the Russell Berrie Nanotechnology Institute (RBNI). We would also like to thank Amit Shocron, Maarten Biesheuvel, and Moran Bercovici for insightful discussions during the preparation of this manuscript.

## ORCID

Rona Ronen https://orcid.org/0000-0001-9361-5431
Matthew E. Suss https://orcid.org/0000-0002-3813-2274

## References

1. K. T. Cho, M. C. Tucker, and A. Z. Weber, "A Review of Hydrogen/Halogen Flow Cells," *Energy Technol.*, **4**(6), 655 (2016).
2. A. Z. Weber, M. M. Mench, J. P. Meyers, P. N. Ross, J. T. Gostick, and Q. Liu, "Redox flow batteries: A review," *J. Appl. Electrochem.*, **41**(10), 1137 (2011).
3. W. A. Braff, M. Z. Bazant, and C. R. Buie, "Membrane-less hydrogen bromine flow battery," *Nat. Commun.*, **4**, 2346 (2013).
4. P Cettou, P. M. Robertson, and N. Ibl, "On the electrolysis of aqueous bromide solutions to bromate," *Electrochim. Acta*, **29**(7), 875 (1984).
5. Y. Zhao, L. Wang, and H. R. Byon, "High-performance rechargeable lithium-iodine batteries using triiodide/iodide redox couples in an aqueous cathode," *Nat. Commun.*, **4**(May), 1896 (2013).
6. M. Skyllas-Kazacos, M. H. Chakrabarti, S. A. Hajimolana, F. S. Mjalli, and M. Saleem, "Progress in Flow Battery Research and Development," *J. Electrochem. Soc.*, **158**(8), R55 (2011).
7. H. Vafiadis and M. Skyllas-Kazacos, "Evaluation of membranes for the novel vanadium bromine redox flow cell," *J. Memb. Sci.*, **279**(1–2), 394 (2006).
8. B. Li and J. Liu, "Progress and directions in low-cost redox-flow batteries for large-scale energy storage," *Natl. Sci. Rev.*, **4**(1), 91 (2017).
9. B. Huskinson, J. Rugolo, S. K. Mondal, and M. J. Aziz, "A High Power Density, High Efficiency Hydrogen-Chlorine Regenerative Fuel Cell with a Low Precious Metal Content Catalyst," *Energy Environ. Sci.*, 8690 (2012).
10. B. Li et al., "Ambipolar zinc-polyiodide electrolyte for a high-energy density aqueous redox flow battery," *Nat. Commun.*, **6**, 6303 (2015).

11. Z. Li, G. Weng, Q. Zou, G. Cong, and Y. C. Lu, "A high-energy and low-cost polysulfide/iodide redox flow battery," *Nano Energy*, **30**, 283 (2016).
12. M. Skyllas-Kazacos, "Novel vanadium chloride/polyhalide redox flow battery," *J. Power Sources*, **124**(1), 299 (2003).
13. B. Huskinson et al., "A metal-free organic-inorganic aqueous flow battery," *Nature*, **505**(7482), 195 (2014).
14. K. T. Cho, P. Albertus, V. Battaglia, A. Kojic, V. Srinivasan, and A. Z. Weber, "Optimization and Analysis of High-Power Hydrogen/Bromine-Flow Batteries for Grid-Scale Energy Storage," *Energy Technol.*, **1**(10), 596 (2013).
15. R. W. Ramette and D. A. Palmer, "Thermodynamics of Tribromide and Pentabromide Anions in Aqueous-Solution," *J. Solution Chem.*, **15**(5), 387 (1986).
16. R. S. Yeo and J. McBreen, "Transport Properties of Nafion Membranes in Electrochemically Regenerative Hydrogen/Halogen Cells," *J. Elecrochem. Soc*, **126**(10), 1682 (1979).
17. W. A. Braff, C. R. Buie, and M. Z. Bazant, "Boundary Layer Analysis of Membraneless Electrochemical Cells," *J. Electrochem. Soc.*, **160**(11), A2056 (2013).
18. T. I. Evans and R. E. White, "A Review of Mathematical Modeling of the Zinc/Bromine Flow Cell and Battery," *J. Electrochem. Soc.*, **134**(11), 2725 (1987).
19. W. C. Hsie and J. R. Selman, "Mass Transport in Supported Zinc Halide Solutions-II. Complexation and Migration Effects," *Electrochim. Acta*, **30**(10), 1381 (1985).
20. K. L. Hawthorne, J. S. Wainright, and R. F. Savinell, "Studies of Iron-Ligand Complexes for an All-Iron Flow Battery Application," *J. Electrochem. Soc.*, **161**(10), A1662 (2014).
21. P. Modiba, M. Matoetoe, and A. M. Crouch, "Electrochemical impedance spectroscopy study of Ce(IV) with aminopolycarboxylate ligands for redox flow batteries applications," *J. Power Sources*, **205**, 1 (2012).
22. J. G. Ibanez, C.-S. Choi, and R. S. Becker, "Aqueous Redox Transition Metal Complexes for Electrochemical Applications as a Function of pH," *J. Electrochem. Soc.*, **134**(12), 3083 (1987).
23. J. Rugolo, B. Huskinson, and M. J. Aziz, "Model of Performance of a Regenerative Hydrogen Chlorine Fuel Cell for Grid-Scale Electrical Energy Storage," *J. Electrochem. Soc.*, **159**(2), B133 (2012).
24. V. Yarlagadda and T. Van Nguyen, "A 1D Mathematical Model of a $H_2/Br_2$ Fuel Cell," *J. Electrochem. Soc.*, **160**(6), F535 (2013).
25. P. K. Adanuvor, R. E. White, and S. E. Lorimer, "Modeling the Rotating Disk Electrode for Studying the Kinetics of Electrochemical Reactions," *J. Electrochem. Soc.*, **134**(3), 625 (1987).
26. M. J. Mader and R. E. White, "A Mathematical Model of a $Zn/Br_2$ Cell on Charge," *J. Electrochem. Soc.*, **133**(7), 1297 (1986).
27. D. A. Saville and O. A. Palusinski, "Theory of Electrophoretic Separations Part I: Formulation of a Mathematical Model," *AlChE J.*, **32**(2), 207 (1986).
28. M. Bercovici, S. K. Lele, and J. G. Santiago, "Open source simulation tool for electrophoretic stacking , focusing , and separation," *J. Chromatogr. A*, **1216**, 1008 (2009).
29. V. Hruška, M. Beneš, J. Svobodová, I. Zusková, and B. Gaš, "Simulation of the effects of complex- formation equilibria in electrophoresis: I. Mathematical model," *Electrophoresis*, **33**(6), 938 (2012).
30. O. Dagan and M. Bercovici, "Simulation tool coupling nonlinear electrophoresis and reaction kinetics for design and optimization of biosensors," *Anal. Chem.*, **86**(15), 7835 (2014).
31. Y. L. Hwang and F. G. Helfferich, "Generalized model for multispecies ion-exchange kinetics including fast reversible reactions," *React. Polym. Ion Exch. Sorbents*, **5**(3), 237 (1987).
32. J. M. Paz-Garcia, J. E. Dykstra, P. M. Biesheuvel, and H. V. M. Hamelers, "Energy from $CO_2$ using capacitive electrodes - A model for energy extraction cycles," *J. Colloid Interface Sci.*, **442**, 103 (2015).
33. J. E. Dykstra, et al., "Theory of ion transport with fast acid-base equilibrations in bioelectrochemical systems," *Physical Review E*, **90**(1), 013302 (2014).
34. R. E. White and S. E. Lorimer, "A Model of the Bromine/Bromide Electrode Reaction at a Rotating Disk Electrode," *J. Electrochem. Soc*, **130**(5), 1096 (1983).
35. M. Štědrý, M. Jaroš, V. Hruška, and B. Gaš, "Eigenmobilities in background electrolytes for capillary zone electrophoresis: III. Linear theory of electromigration," *Electrophoresis*, **25**(18–19), 3071 (2004).
36. K.-M. Yen, T. Yeu, and R. E. White, "A Mathematical Model of Electrochemical Reactions Coupled with Homogeneous Chemical Reactions," *J. Electrochem. Soc.*, **138**(4), 1051 (1991).
37. T. I. Evans and R. E. White, "A Mathematical Model of a Zinc/Bromine Flow Cell," *J. Electrochem Soc*, **134**(4), 866 (1987).
38. K. Oh, A. Z. Weber, and H. Ju, "Study of bromine species crossover in $H_2/Br_2$ redox flow batteries," *Int. J. Hydrogen Energy*, **42**(6), 3753 (2017).
39. M. Tedesco, H. V. M. Hamelers, and P. M. Biesheuvel, "Nernst-Planck transport theory for (reverse) electrodialysis: I. Effect of co-ion transport through the membranes channel," *J. Memb. Sci.*, **510**, 370, (2016).
40. A. A. Sonin and R. F. Probstein, "A hydrodynamic theory of desalination by electrodialysis.," *Desalination*, **5**, 293 (1968).
41. M. E. Suss, K. Conforti, L. Gilson, C. R. Buie, and M. Z. Bazant, "Membraneless flow battery leveraging flow- through heterogeneous porous media for improved power density and reduced crossover," *RSC Adv.*, **6**, 100209 (2016).
42. J. E. Dykstra, K. J. Keesman, P. M. Biesheuvel, and A. van der Wal, "Theory of pH changes in water desalination by capacitive deionization," *Water Res.*, **119**, 178 (2017).
43. V. Livshits, A. Ulus, and E. Peled, "High-power $H_2/Br_2$ fuel cell," *Electrochem. commun.*, **8**(8), 1358 (2006).
44. D. P. Scamman, G. W. Reade, and E. P. L. Roberts, "Numerical modelling of a bromide-polysulphide redox flow battery. Part 1: Modelling approach and validation for a pilot-scale system," *J. Power Sources*, **189**(2), 1220 (2009).
45. P. K. Adanuvor, R. E. White, and S. E. Lorimer, "The Effect of the Tribromide Complex Reaction on the Oxidation/Reduction Current of the $Br_2/Br^-$ Electrode," *J. Electrochem. Soc.*, **134**(6), 1450 (1987).